

Coherent Integration Algorithm for Weak Maneuvering Target Detection in Passive Radar Using Digital TV Signals

Ying Zhou^(✉), Weijie Xia, Jianjiang Zhou, Linlin Huang,
and Minling Huang

Laboratory of Radar Imaging and Microwave Photonics,
College of Electronic and Information Engineering, Ministry of Education,
Nanjing University of Aeronautics and Astronautics, Nanjing 211100, China
{nuaazhouying, nuaaxwj, zjjee}@nuaa.edu.cn

Abstract. This paper considers the coherent integration problem of detecting weak maneuvering targets in passive radar using digital television terrestrial broadcasting (DTTB) signals. By dividing the continuous DTTB echoes into multiple segments, the generalized Radon-Fourier transform (GRFT) which was proposed to realize coherent integration of maneuvering targets for pulse Doppler radar can be utilized in DTTB-based passive radar. The GRFT can obtain ideal coherent integration gain but suffers a heavy computational burden. In this paper, a fast implementation algorithm of GRFT using the modified wind driven optimization (MWDO) is proposed. Compared with the existing particle swarm optimization (PSO) method, the proposed method can achieve better detection performance with a similar computational cost in DTTB-based passive radar. Several numerical experiments are also provided to demonstrate the effectiveness of the proposed method.

Keywords: Weak maneuvering target detection · Passive radar
Generalized Radon-Fourier Transform (GRFT)
Wind Driven Optimization (WDO)

1 Introduction

Passive bistatic radar often uses non-cooperative civil radiation sources to detect and locate targets. Compared with the traditional monostatic radar, passive radar has several attractive advantages such as stronger survivability, better anti-jamming ability and potential anti-stealth capacity [1]. Among various illuminators, digital television terrestrial broadcasting (DTTB) signals are better choices for passive radar due to the high power, wide coverage, and higher range resolution.

It is known that pulses integration especially coherent integration can greatly improve the radar detection performance. The traditional coherent integration method for DTTB-based passive radar is to compute the cross-ambiguity function (CAF) [2]. However, the computational burden of CAF is heavy and the integration performance via CAF will be greatly influenced by the range migration (RM) and the Doppler frequency migration (DFM) which are caused by the maneuvering motions of targets

[3]. To reduce the computational complexity, a signal segmentation method [1] can be utilized. After segmentation, the continuous DTTB signal have equivalent fast time and slow time, which is similar to pulse signal in pulse Doppler radar.

In pulse Doppler radar, the commonly used integration method is moving target detection (MTD) [4], but it will become invalid when RM occurs. Regarding this, Zhang and Zeng [5] have proposed to perform keystone transform (KT) to deal with RM before MTD. However, traditional KT can only correct the first-order RM caused by the velocity of targets. Li et al. [6, 7] have proposed a fast coherent integration method based on adjacent cross correlation function (ACCF) for maneuvering targets. This method can remove the RM and reduce the order of DFM and is free of parameters searching. Unfortunately, ACCF cannot be applied to DTTB-based passive radar because of the pseudo random characteristics of DTTB signals. In recent years, generalized Radon-Fourier transform (GRFT) [8] has been proposed to achieve ideal coherent integration of maneuvering targets via jointly searching in parameter space, but it suffers a heavy computational burden. Through converting the realization of GRFT into an optimization problem, Qian et al. [9] proposed an improved particle swarm optimization (PSO) method to fast implement GRFT.

Although PSO greatly reduces the computational burden of GRFT, it suffers an apparent detection performance loss. For the purpose of improving the detection performance, this paper proposes a fast implementation algorithm of GRFT based on the modified wind driven optimization (MWDO). Compared with PSO, MWDO can achieve better detection performance with similar computational cost in DTTB-based passive radar.

2 Signal Model and Signal Segmentation Method

2.1 Signal Model of Passive Radar

Figure 1 depicts the bistatic passive radar geometry. The baseline runs from the transmitter Tx to the passive radar receiver Rx, and they are separated by the base-length L . Suppose that the target is located at O at the initial time and moves to O' at time t . The distance between the target and the transmitter at the initial time and time t is denoted by R_{T0} and $R_T(t)$ respectively while the distance between the target and the receiver at the initial time and time t is denoted by R_{r0} and $R_r(t)$ respectively. β is the bistatic angle at the initial time and φ denotes the movement direction of the target. The DTTB source transmits the signal $s(t)$. The passive radar receiver collects both a reference signal $x(t)$ via a line-of-sight (LOS) path direct from the illuminator, and a surveillance signal $s_r(t)$ reflected via the target of interest. $s_r(t)$ has a time delay $\tau = R(t)/c$ refers to $x(t)$, where

$$R(t) = R_T(t) + R_r(t) - L \quad (1)$$

The received radar echo can be denoted as

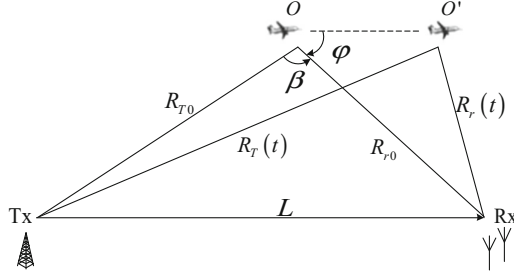


Fig. 1. Sketch map of the bistatic structure of passive radar.

$$s_r(t) = A_e s(t - R(t)/c) \exp(-j2\pi f_c R(t)/c) \quad (2)$$

where c is the speed of light, A_e is the amplitude, and f_c is the carrier frequency.

Assume that the target moving from O to O' is maneuvering. Neglecting the high order components, the instantaneous range $R_m(t)$ between O and O' can be denoted as

$$R_m(t) = v_0 t + \frac{1}{2} a_0 t^2 + \frac{1}{6} g_0 t^3 \quad (3)$$

where v_0 , a_0 and g_0 denotes respectively the velocity, acceleration and jerk of the target. From the geometric relationship of Fig. 1, we can obtain that

$$R_T(t) = \sqrt{R_{T0}^2 + R_m^2(t) - 2R_{T0}R_m(t) \cos(\beta + \varphi)} \quad (4)$$

$$R_r(t) = \sqrt{R_{r0}^2 + R_m^2(t) - 2R_{r0}R_m(t) \cos(\varphi)} \quad (5)$$

Then, inserting (4) and (5) into (1) and expanding (1) into Taylor series at $t = 0$, we have

$$\begin{aligned} R(t) = \alpha_0 - \alpha_1 t - \alpha_2 t^2 - \alpha_3 t^3 \approx R_{T0} + R_{r0} - L - \left[2v_0 \cos\left(\varphi + \frac{\beta}{2}\right) \cos\frac{\beta}{2} \right] t \\ - \left[a_0 \cos\left(\varphi + \frac{\beta}{2}\right) \cos\frac{\beta}{2} \right] t^2 - \left[\frac{1}{3} g_0 \cos\left(\varphi + \frac{\beta}{2}\right) \cos\frac{\beta}{2} \right] t^3 \end{aligned} \quad (6)$$

Higher order components are ignored. α_0 is the relative initial range and α_1 , α_2 and α_3 are the relative motion parameters.

The reference signal $x(t)$ can be simply expressed as a direct path (DP) component from the transmitter and the short delay is neglected for simplicity, i.e.

$$x(t) = A_r s(t) \quad (7)$$

where A_r is the amplitude of the received reference signal. In this paper, it is assumed that the multipath clutter has been preprocessed.

2.2 Signal Segmentation Method

The segmentation method is shown in Fig. 2. First, the number of segments can be determined according to the maximum relative velocity of the target required to be detected by the passive radar system, i.e.

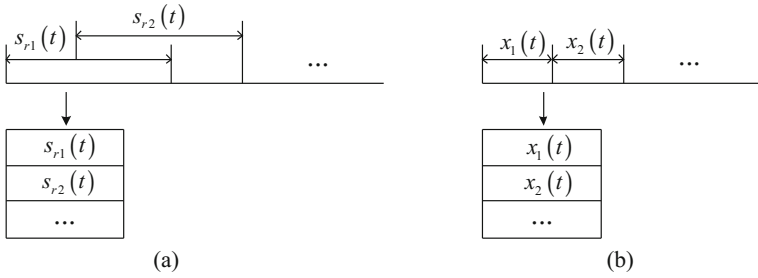


Fig. 2. Schematic diagram of signal segmentation method. (a) Segmentation method for echo signal. (b) Segmentation method for reference signal.

$$N = 2v_{\max}T/\lambda \tag{8}$$

where T is the integration time and λ is the wavelength. In this way, the Doppler ambiguity can be avoided. Then the efficient length of each segment of the reference signal is $L_r = L/N$, where L is the total signal length. In order to guarantee the expected detection range, the overlapping segmentation method is utilized for the echo signal. The segment length of echo signal is $L_e = L_r + f_s R_{\max}/c$, and R_{\max} denotes the maximum relative range required to be detected by radar. At last, pad zeros for the segmented reference signal to insure that the length of each segment of reference signal and echo signal is equal.

After segmentation, $T_r = L_r/f_s$ can be considered as the pulse repetition interval. Then the equivalent pulse compression can be calculated as

$$s_{pc}(t_m, \hat{t}) = A' s'(\hat{t} - R(t_m)/c) \exp\left(-j \frac{2\pi}{\lambda} R(t_m)\right) \tag{9}$$

where \hat{t} is the fast time, $t_m = mT_r$ ($m = 0, 1, \dots, N - 1$) is the slow time, $s'(t)$ is the inverse Fourier transform result of $|S(f)|^2$, $S(f)$ stands for the Fourier transform of the transmitted signal $s(t)$, $A' = A_e A_r$, and $R(t_m) = \alpha_0 - \alpha_1 t_m - \alpha_2 t_m^2 - \alpha_3 t_m^3$.

From (9), it's easy to see that the target envelope varies with t_m and the phase is also the cubic function of t_m . The changes of envelope and phase will easily result in RM and DFM. For the purpose of coherently accumulating the target's energy, both the RM and the DFM are required to be compensated [10].

3 Coherent Integration via MWDO

3.1 Definition and Analysis of GRFT

GRFT is a coherent integration algorithm via jointly searching in multi-dimensional parameter space. The definition of GRFT in [8] is given as follows:

Suppose a 2D complex function $f(t_m, \hat{t}) \in C$ is defined in the (t_m, \hat{t}) plane and a parameterized P -dimensional function $\hat{t} = \eta(t_m; \hat{\alpha}^P)$ is used for searching a certain time-varied curve in the plane, where $\hat{\alpha}^P = [\hat{\alpha}_0, \hat{\alpha}_1, \dots, \hat{\alpha}_{P-1}]$. Then GRFT can be defined as

$$G(\hat{\alpha}^P) = \int_{-\infty}^{\infty} f(t_m, \eta(t_m; \hat{\alpha}^P)) \exp(j2\pi\varepsilon\eta(t_m; \hat{\alpha}^P)) dt_m \quad (10)$$

where ε is a known constant with respect to $\eta(t_m; \hat{\alpha}^P)$.

Let $f(t_m, \hat{t}) = s_{pc}(t_m, \hat{t})$, then (10) can be rewritten as

$$G(\hat{\alpha}^P) = \int_{-\infty}^{\infty} s_{pc}(t_m, \hat{t}(t_m)) \exp(j2\pi f_c \hat{t}(t_m)) dt_m \quad (11)$$

where $\hat{t}(t_m) = \frac{1}{c} \sum_{p=0}^{P-1} \hat{\alpha}_p t_m^p$. When the searching values of motion parameters $[\hat{\alpha}_0, \hat{\alpha}_1, \dots, \hat{\alpha}_{P-1}]$ match with the target's real motion values $[\alpha_0, \alpha_1, \dots, \alpha_{P-1}]$, the ideal coherent integration gain could be achieved, that is $G(\hat{\alpha}^P) = NA'$. Then the target can be detected and the motion parameters can be easily obtained by the location of the peak in the parameter space.

In pulse Doppler radar, the blind speed side lobe (BSSL) [11] will appear in GRFT because of limited integration time, Doppler ambiguity, discrete pulse sampling, and finite range resolution, which will cause serious false alarms. In DTTB-based passive radar, the Doppler ambiguity can be avoided by using flexible segmentation method, so the BSSL phenomenon can also be avoided in GRFT.

3.2 Modified Wind Driven Optimization

The model of wind driven optimization (WDO) is based on the definition of trajectories of small air parcels within the earth atmosphere [12]. In WDO, a population of air parcels is distributed throughout a N -dimensional problem space, and the velocity of air parcels is updated in each iteration process based on the equation which is derived from Newton's second law of motion and the ideal gas laws. It is given by

$$\mathbf{U}_{new} = (1 - \alpha)\mathbf{U}_{cur} - g\mathbf{X}_{cur} + [RT|1/i - 1|(\mathbf{X}_{opt} - \mathbf{X}_{cur})] + (C\mathbf{U}_{cur}^{other \dim}/i) \quad (12)$$

where i represents the rankings of the air parcels. Equation (12) demonstrates that the updated velocity \mathbf{U}_{new} for the next iteration process is associated with the current velocity \mathbf{U}_{cur} , the current position \mathbf{X}_{cur} , the optimal position \mathbf{X}_{opt} with the highest

pressure value that has been found until the current iteration, the current velocity $\mathbf{U}_{cur}^{other \ dim}$ which is randomly chosen from other dimensions, and the four coefficients α , g , RT , and C . The position of air parcel can be updated by

$$\mathbf{X}_{new} = \mathbf{X}_{cur} + \mathbf{U}_{new} \quad (13)$$

WDO provides extra degrees of freedom to fine tune in the velocity update equation compared with PSO, which indicates a better optimization capacity. As illustrated in [12], the optimum performance of WDO can be achieved by selecting proper values for the four coefficients, but the optimum values of the WDO coefficients may vary from problem to problem. Considering the problem, we propose the modified WDO (MWDO) to tune the four coefficients in each iteration process by random distributions. The values of coefficients are given by

$$\alpha = RT = g = 0.1 * rand_L \quad (14)$$

$$C = 2.5 * rand_U \quad (15)$$

where the random number $rand_U$ is uniformly distributed between 0 and 1, and the random number $rand_L$ is subject to Levy distribution [13]. Its probability density function over the domain $x \geq \mu$ is

$$f(x; \mu, \gamma) = \sqrt{\frac{\gamma}{2\pi}} \frac{e^{-\frac{\gamma}{2(x-\mu)}}}{(x-\mu)^{3/2}} \quad (16)$$

where γ is the scale parameter and μ is the location parameter. In this paper, $\mu = 0$ and $\gamma = 0.001$ are selected.

By applying MWDO, the optimization ability of WDO in a noisy environment can be enhanced and at the same time, the difficulty in choosing proper coefficients in WDO can be overcome.

3.3 Fast Implementation of GRFT via MWDO

GRFT can be fast implemented via MWDO. The whole target detection procedure based on MWDO in DTTB-based passive radar is shown in Fig. 3 and the detailed description of the proposed method is given as follows:

- Step 1. Specify the basic parameters in MWDO, including the population size S , the maximum number of iteration k_{max} , the dimension of the searching space, the searching range of each parameter, and the restrictions on velocities of air parcels.
- Step 2. Initialize air parcels' locations and velocities.
- Step 3. Sort air parcels based on their pressure values. In GRFT, pressure value refers to the absolute value of GRFT, denoted by $|G(\mathbf{X})|$.
- Step 4. Generate the values of coefficients of MWDO via (14) and (15).
- Step 5. Update the velocities and locations of air parcels via (12) and (13).

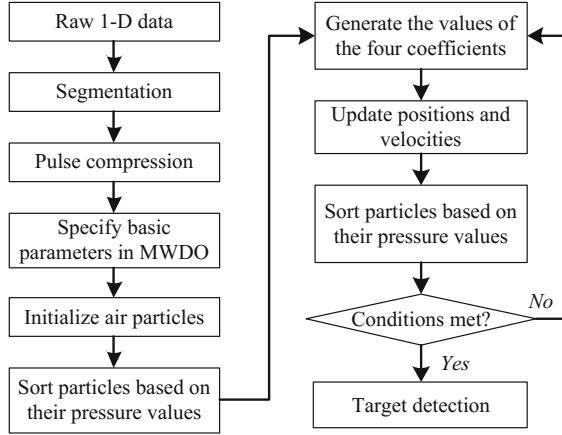


Fig. 3. Flow chart of the target detection method in DTTB-based passive radar.

Step 6. Sort these updated air parcels based on their pressure values and find the current optimal air parcel $\mathbf{X}_{opt}(k)$.

Step 7. Repeat Step 4 to Step 6 until one of the following conditions is met:

- (1) $|G(\mathbf{X}_{opt}(k))| > \gamma$ and $k \leq k_{max}$;
- (2) $|G(\mathbf{X}_{opt}(k))| \leq \gamma$ and $k > k_{max}$.

The parameter γ is the detection threshold calculated from the preset false alarm probability. When condition 1 is met, the target is detected and when condition 2 is met, the radar system tells that there is no target.

4 Numerical Results

In this section, numerical experiments are provided to demonstrate the effectiveness of the proposed fast implementation method of GRFT. The DTTB-based passive radar parameters are listed in Table 1.

Table 1. Simulation parameters of DTTB-based passive radar.

Signal mode	Bandwidth	Carrier frequency	Integration time
Single-carrier mode	7.56 MHz	674 MHz	0.22 s

4.1 Detection Performance

The detection performances of traditional ergodic-search GRFT, PSO-based GRFT, MWDO-based GRFT, KT, and MTD are investigated via Monte Carlo trials. The false alarm probability is $P_{fa} = 10^{-6}$. The population size $S = 150$ and the maximum number of iteration $k_{max} = 800$ are specified for PSO and MWDO. The relative initial

range and the relative maneuvering motion parameters of the target are given as follows: $\alpha_0 = 150$ km, $\alpha_1 = 800$ m/s, $\alpha_2 = 90$ m/s², and $\alpha_3 = 10$ m/s³. Figure 4 shows the detection probabilities of the five detectors versus different SNR values. Figure 4 demonstrates that the proposed MWDO-based GRFT is superior to PSO-based GRFT but still suffers detection performance loss compared with the traditional GRFT. The reason is that MWDO is a stochastic optimization method and it cannot jump out of the convergence to noise peaks each time. The detection performance loss of MWDO is the cost of the reduced computational complexity.

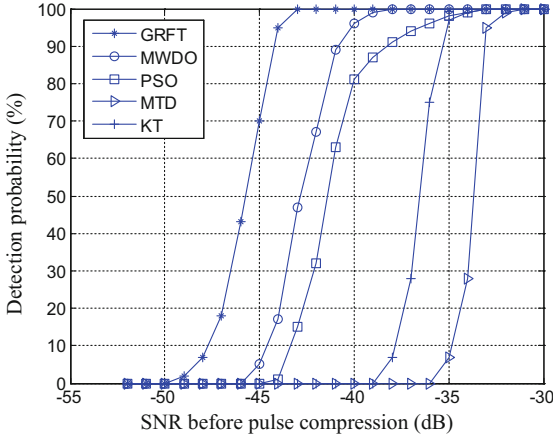


Fig. 4. Detection probability of GRFT, MWDO, PSO, KT, and MTD.

4.2 Computational Cost

Denote the number of range cells, pulses, and searching motion parameters $\alpha_p (p = 1, 2, 3, \dots, P - 1)$ by M, N, N_p , respectively. Then $\prod_{p=1}^{P-1} NN_p$ searches are needed

and the computational complexity is $O\left(\prod_{p=1}^{P-1} MNN_p\right)$ for the traditional GRFT [14].

While only k_{\max} searches are needed for MWDO and PSO if they are terminated when the number of iteration reaches k_{\max} . In fact, when condition 1 in Step 7 is met, the two algorithms can be terminated earlier. The running time of the traditional GRFT, MWDO-based GRFT, and PSO-based GRFT under different motion orders is shown in Fig. 5. From Fig. 5 we can see that with the increase of the motion order, the time cost of GRFT grows nearly exponentially while the running time of MWDO and PSO stays stable. The computational complexity of MWDO is slightly higher than PSO due to the additional sorting process of air parcels, which is acceptable. It is obvious that when the motion order equals to 3, the computational complexity of intelligent optimization algorithms is far less than that of the ergodic-search GRFT, which validates the physical realizability of the proposed algorithm.

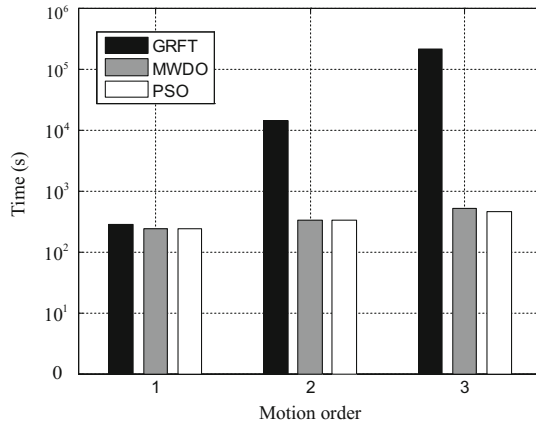


Fig. 5. Computational cost of the ergodic-search GRFT, MWDO, and PSO.

5 Conclusions

This paper deals with the coherent integration problem of the weak maneuvering target in passive radar using DTTB signals. By designing suitable signal segmentation method, GRFT can be applied to achieve ideal integration performance by correcting RM and DFM at the same time in passive radar. Then a fast implementation method for GRFT is proposed to reduce the computational burden, namely MWDO. Compared with the ergodic-search GRFT, MWDO requires much lower computational load, which means it can realize the maneuvering target detection in a much more efficient way. Compared with the existing PSO method, MWDO has better detection performance with a similar computational complexity. It should be noticed that although MWDO has stronger anti-noise ability, it still suffers some detection performance loss, which is the cost of the reduced computational burden. Finally, several simulation experiments are provided to validate the effectiveness of the proposed method. Future work may further improve the proposed method and extend it to multi-target detection.

Acknowledgments. The work was supported by the National Natural Science Foundation of China (Grant no. 61201366), the Fundamental Research Funds for the Central Universities (Grant no. NS2016040), the Fundamental Research Funds for the Central Universities (Grant no. NJ20150020), and the Priority Academic Program Development of Jiangsu Higher Education Institutions.

References

1. Tao, S., Liu, S.H., et al.: Efficient architecture and hardware implementation of coherent integration processor for digital video broadcast-based passive bistatic radar. *IET Radar Sonar Navig.* **10**(1), 97–106 (2016)
2. Tao, R., Zhang, W.Q., Chen, E.Q.: Two-stage method for joint time delay and Doppler shift estimation. *IET Radar Sonar Navig.* **2**(1), 71–77 (2008)

3. Chen, X.L., Guan, J., Liu, N.B., et al.: Maneuvering target detection via Radon-Fractional Fourier transform-based long-time coherent integration. *IEEE Trans. Signal Process.* **62**(4), 939–953 (2014)
4. Skolnik, M.I.: Introduction to radar system, 3rd edn. Mc-Graw-Hill, New York (2002)
5. Zhang, S.S., Zeng, T.: Weak target detection based on keystone transform. *Acta Electron. Sinica.* **33**(9), 1675–1678 (2005)
6. Li, X.L., Cui, G.L., Kong, L.J., et al.: Fast non-searching method for maneuvering target detection and motion parameters estimation. *IEEE Trans. Signal Process.* **64**(9), 2232–2244 (2016)
7. Li, X.L., Cui, G.L., Yi, W.: A fast maneuvering target motion parameters estimation algorithm based on ACCF. *IEEE Sig. Process. Lett.* **22**(3), 270–274 (2015)
8. Xu, J., Yu, J., Peng, Y.N., et al.: Radon-Fourier transform for radar target detection, I: generalized Doppler filter bank. *IEEE Trans. Aerosp. Electron. Syst.* **47**(2), 1186–1202 (2011)
9. Qian, L.C., Xu, J., Xia, X.G., et al.: Fast implementation of generalized Radon-Fourier transform for maneuvering radar target detection. *Electron. Lett.* **48**(22), 1427–1428 (2012)
10. Chen, X.L., Huang, Y., Liu, N.B., et al.: Radon-fractional ambiguity function-based detection method of low-observable maneuvering target. *IEEE Trans. Aerosp. Electron. Syst.* **51**(2), 815–833 (2015)
11. Xu, J., Yu, J., Peng, Y.N., et al.: Radon-Fourier transform (RFT) for radar target detection (II): blind speed sidelobe suppression. *IEEE Trans. Aerosp. Electron. Syst.* **47**(4), 2473–2489 (2011)
12. Bayraktar, Z., Komurcu, M., Werner, D.H.: The wind driven optimization technique and its application in electromagnetics. *IEEE Trans. Antennas Propag.* **61**(5), 2745–2757 (2013)
13. Liang, Y.J., Chen, W.: A survey on computing Levy stable distribution and a new MATLAB toolbox. *Sig. Process.* **93**(1), 242–251 (2013)
14. Xu, J., Xia, X.G., Peng, S.B., et al.: Radar maneuvering target motion estimation based on generalized Radon-Fourier transform. *IEEE Trans. Sig. Process.* **60**(12), 6190–6201 (2012)